Princeton Plasma Physics Laboratory

PPPL-

PPPL-

Princeton Plasma Physics Laboratory
Report Disclaimers

Full Legal Disclaimer

Trademark Disclaimer

PPPL Report Availability

Princeton Plasma Physics Laboratory:

http://www.pppl.gov/techreports.cfm

Office of Scientific and Technical Information (OSTI):

http://www.osti.gov/bridge

Related Links:

U.S. Department of Energy

Office of Scientific and Technical Information

Fusion Links

Excitation of Alfvén Modes by Energetic Particles in Magnetic Fusion

N.N. Gorelenkov

PPPL, Princeton University

Abstract. Ions with energies above the plasma ion temperature (also called super thermal, hot or energetic particles - EP) are utilized in laboratory experiments as a plasma heat source to compensate for energy loss. Sources for super thermal ions are direct injection via neutral beams, RF heating and fusion reactions. Being super thermal, ions have the potential to induce instabilities of a certain class of magnetohydrodynamics (MHD) cavity modes, in particular, various Alfvén and Alfvén-acoustic Eigenmodes. It is an area where ideal MHD and kinetic theories can be tested with great accuracy. This paper touches upon key motivations to study the energetic ion interactions with MHD modes. One is the possibility of controlling the heating channel of present and future tokamak reactors via EP transport. In some extreme circumstances, uncontrolled instabilities led to vessel wall damages. This paper reviews some experimental and theoretical advances and the developments of the predictive tools in the area of EP wave interactions. Some recent important results and challenges are discussed. Many predicted instabilities pose a challenge for ITER, where the alpha-particle population is likely to excite various modes.

Keywords: Alfvén waves, energetic particles, magnetic fusion.

I. INTRODUCTION

This lecture paper is based on the material presented in the course of a student lecture given at the International ITER Summer School (IISS 2011) held in Cadarache, France. It is written to summarize in the introductory form some key achievements obtained in the area of EP (Energetic Particle) related physics. This paper is far from an overview, but gives an idea on the achieved progress. The key topics covered are single particle confinement, classical distribution function, instabilities due to EPs, EP modeling using methods ranging from the initial value codes to more sophisticated numerical codes, applications of such codes to EP instabilities in present-day tokamaks and finally applications to ITER plasma expected to be near burning conditions. Other effects due to EPs are important and are covered in other publications of these proceedings.

EPs play an important role in present-day experiments. They are key to the main controllable mechanisms of plasma heating of thermonuclear plasma. As such three main sources of EPs are known and widely used. They are neutral beam injection (NBI), ion cyclotron resonant heating (ICRH) particles, and energetic fusion products (α's, protons, T and so on).

Because of their importance to near-burning plasma conditions, EPs attracted the attention of plasma scientists since the field was established. Initially EPs were argued to excite the so-called "thermonuclear" instabilities with the following publication among the first (and seminal) on this subject [1]. As the field grew many papers and some reviews

were published. Some are listed in this paper, which should be helpful for the introductory purpose [2–6]. Recently many people further acknowledged the progress in the EP physics and some other reviews appeared [7–9].

The purpose of this paper is to highlight some aspects that are poorly covered by the published reviews, but seem to be important for the EP field. In particular, this lecture highlights the topics interesting for the young reseacher working as a numerical simulator.

II.   SINGLE PARTICLES CONFINEMENT AND THEIR DISTRIBUTION FUNCTION

The single particle confinement of EPs is similar to any other particle motion and is covered well by the drift theories [2]. The EP peculiarities may come from the practical energies used in fusion experiments worldwide, which are by default (for the purpose of plasma heating) much higher than the thermal ion temperature,

$$\mathcal{E}_h \gg T_{i,e}. \tag{1}$$

Because of this it can be shown that the EPs are affected primarily by the collisional drag from thermal electrons with relatively moderate pitch angle scattering on thermal ions. As a result, the EP distribution function (DF) is formed slowing down from the injection energy (for NBI ions, or birth energy for fusion products) down to the characteristic thermal energy, which is close to the plasma temperature. If the plasma temperature is low the pitch angle scattering can be neglected and particle pitch angle remains almost constant so that

$$\lambda = \frac{\mu B_0}{\mathcal{E}_h} = const. \tag{2}$$

As the EP drifts, its motion is characterized by the conservation of its canonical integral, which is the toroidal moment and is given by the drift theory:

$$P_\varphi = \frac{\omega_c \psi}{B 2\pi} - v_\varphi R. \tag{3}$$

In this limit we find that the DF is a function of constants of motion (COM), which are the aforementioned variables plus the particle velocity, v:

$$f_h = f_h \left(v, P_\varphi, \lambda, t \right) = \frac{S_\alpha \left(\bar{\psi}, t \right) \tau_s v_0^2 H \left(v - v_0 \right)}{4\pi \left(v^3 + v_*^3 \right)}, \tag{4}$$

where S_α is the source of EPs or fusion alphas, and $H(x)$ is a Heaviside step-function, $= 0$ at $x < 0$, $= 1$ at $x > 0$. Here we introduced a time averaged magnetic flux over the particle orbit, which is by itself a function of COM. We note that the DF in the form of Eq.(4) is a very good approximation as the particle source is evaluated at $\bar{\psi}$. More sophisticated distribution is a solution found by solving the drift kinetic equation (see for example Ref.[10])

$$\frac{\partial f_h}{\partial t} - \frac{1}{\tau_{se} v^2} \frac{\partial}{\partial v} \left(v^3 + v_*^3 \right) f_h + \frac{f_h}{\tau_{loss}} - S_\alpha = 0, \tag{5}$$

where we added the loss term in a general form characterized by the loss time, τ_{loss}.
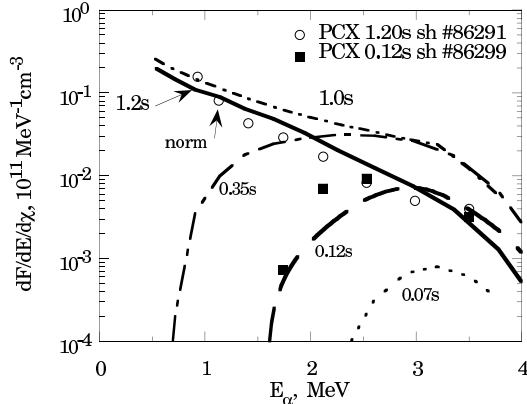
Figure 1: *Measured (points) and modeled (lines) α-particle distribution function in TFTR beam blip experiments. Shown are the distribution functions measured in two different similar TFTR discharges. The measurements are compared with the simulations taken at the consequent times.*

EP DF with the effect of particle losses follows directly from the last equation:

$$f = \frac{Cn_b H}{v^3 + v_*^3} \left(\frac{v^3 + v_*^3}{v_{b0}^3 + v_*^3} \right)^{\tau_{se}/3\tau_{loss}},$$

which then transformed into a steady state function if the loss time goes to infinity, i.e. $f \sim 1/\left(v^3 + v_*^3\right)$ if $\tau_{loss} \to \infty$.

It turned out that the formation of the distribution function, such as in Eq.(4), was checked experimentally in TFTR DT (deuterium-tritium) experiments. In those experiments a special diagnostic, Pellet Charge eXchange (PCX) [11], was installed, which allowed instant single pitch angle measurements of the velocity spectrum of fusion alphas in different radial locations. The PCX diagnostic was a powerful tool and presented a lot of valuable data during the series of DT and DD experiments on TFTR as well as on JET.

In one particular series of TFTR experiments [10] PCX measured fusion α-particle distribution function locally at different times after the injection. The results are illustrated in Fig. 1, where the measured points are compared with the expectations followed from the numerical simulations using the FPPT (Fokker-Planck post TRANSP processor) code.

III.   ALFVÉNIC MODES IN FUSION RESEARCH

Alfvén oscillations are natural and arguably one of the most fundamental types for the fusion plasma close to burning conditions. They are capable of resonant interactions with EPs. The reason for this is remarkable and has to do with the characteristic energetic particle velocities, which, as can be shown, are well above the plasma ion thermal speed. At the same time the Alfvén speed must be high enough to ensure relatively low plasma pressure, i.e.,

$$\beta_i = \frac{8\pi n_i T_i}{B^2} = \frac{v_i^2}{v_A^2} \simeq 0.1 \sim O\left(\epsilon\right) \ll 1, \tag{6}$$

where v_A is the local Alfvén velocity. The latter is required from the macroscopic stability point of view. It turns out that both the Alfvén speed and EP velocity must be above the thermal one, which often requires their proximity and implies a possibility of a resonance.

This was realized first theoretically and later was confirmed experimentally. As mentioned, the beginning of the research on fast ions can be arguably traced back to such papers as Refs.[1, 12], where the authors focused on the superalfvenic nature of the energetic particle component in a future fusion tokamak reactor. Studied instabilities due to EPs were called thermonuclear. The researchers did not pursue those lines of arguments in subsequent research for different reasons. One of them was that there were no cavity modes known to the theory, which could be responsible for releasing energy associated with the fast ions. Instead they looked at the local instabilities.

Only after the new discoveries, which showed theoretically that the Alfvénic cavity modes exist could the scientists seriously consider the new family of eigenmodes. This new family has to do with the way the poloidal harmonics of the Alfvén waves couple together in order to form the coherent radially trapped structures. The modes associated with such coupled harmonics were called toroidicity-induced Alfvén eigenmodes (TAE).

A. Alfvén continuum concept is a key for addressing eigenmode problems

The concept of the Alfvén continuum (AC) (see for example [13, 14]) is instrumental in addressing the eigenmode problem. It is a concept used widely in plasma theory in order to identify the region of the plasma where the ideal MHD equations have a singularity or, in other words, where the local shear Alfvén wave exists given the peculiarities of the geometrical bounds of a wavevector. In a simple case of a homogeneous plasma such a local solution can be schematically written as

$$\omega = \omega_A = k_\parallel v_A, \tag{7}$$

where $k_\parallel$ is the parallel component of the wavevector of a propagating wave. If the plasma carries the current and is essentially nonuniform, $\omega_A(r)$ provides the continuum functional dependence. In realistic plasma geometry of a tokamak any oscillation can be expanded in terms of the poloidal harmonics

$$\xi = \sum_m \xi_m e^{-i\omega t + i k_m x} = e^{-i\omega t - in\varphi} \sum_m \xi_m e^{im\theta}, \tag{8}$$

where we introduced m and n the poloidal and toroidal mode numbers. For such a form of the perturbations one can obtain the parallel wavevector component expression as $k_\parallel \simeq (m - nq)/qR$ with $q(r) \simeq r B_\varphi / R B_\theta$.

It is instructive to show AC in a given geometry and the possibility to use its conceptual properties, which are being routinely exploited in the analysis of problems aimed at studies of the Alfvén eigenmodes. In addition to the Alfvén continuum people often use the acoustic (or sonic) continuum (which is another fundamental MHD oscillation) and in the following illustration we consider both.

If one considers the plasma in a cylinder and makes use of the representation, Eq.(8), the simplified picture emerges with the uncoupled set of continuum dependencies, which are shown in Fig. 2a. Both Alfvénic and acoustic continua are shown (here we follow the arguments given in Ref.[15]). Each point on each curve in this figure corresponds to the singular behavior of a corresponding harmonic. Note that we show schematically both continua typical for a laboratory plasma case when the acoustic (subscript s for sonic) velocity, $v_s^2 = v_A^2 \gamma \beta_{pl}/2$, is much smaller than the Alfvénic one, where $\beta_{pl} \ll 1$ and γ is the specific heat ratio.
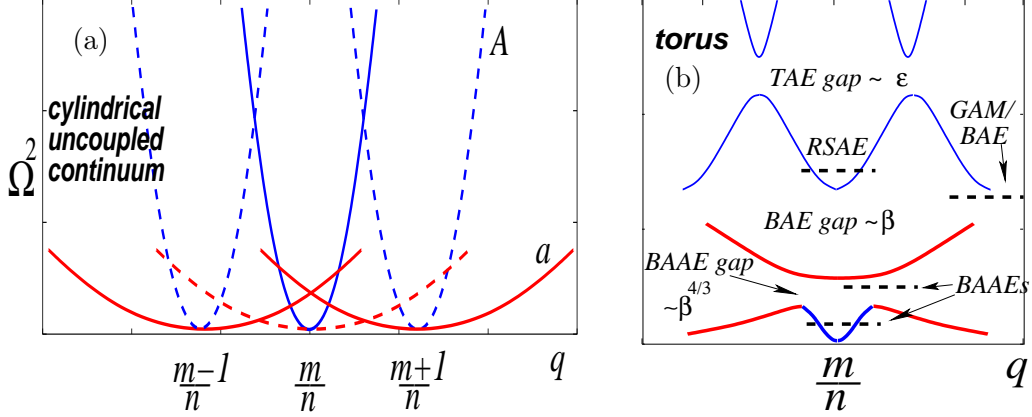
4

Figure 2: *Schematic of the low-frequency Alfvénic and acoustic continua in a cylinder (a) and in a torus (b).*

A more rigorous theory can be developed within the ideal MHD formulation where both continua are coupled [14, 16]. The system can be derived, which combines two equations

$$\omega^2 \rho \frac{|\nabla \psi|^2}{B^2} \xi_s + (\mathbf{B} \cdot \nabla) \frac{|\nabla \psi|^2}{B^2} (\mathbf{B} \cdot \nabla) \xi_s + \gamma p k_s \nabla \cdot \vec{\xi} = 0,$$

$$\left(\frac{\gamma p}{B^2} + 1 \right) \nabla \cdot \vec{\xi} + \frac{\gamma p}{\omega^2 \rho} (\mathbf{B} \cdot \nabla) \frac{\mathbf{B} \cdot \nabla}{B^2} \nabla \cdot \vec{\xi} + k_s \xi_s = 0, \tag{9}$$

where ψ is the poloidal magnetic flux, ρ is the plasma density, $\xi_s \equiv \vec{\xi} \cdot [\mathbf{B} \times \nabla \psi] / |\nabla \psi|^2$, $\vec{\xi}$ is the plasma displacement, $k_s \equiv 2\mathbf{k} \cdot [\mathbf{B} \times \nabla \psi] / B^2$ and $\mathbf{k}$ and $\mathbf{B}$ are vectors of the magnetic curvature and field. Alfvén-acoustic wave coupling, which may lead to the formation of the continuum and the global modes in toroidal geometry, follows from the tokamak ordering limit. We then find that the expression for the geodesic curvature is $k_s = 2\varepsilon \sin \theta / q$, where $\varepsilon = r/R \ll 1$ and we neglect corrections of order $O(\varepsilon^2)$ and higher. This is justified for the low mode frequency, such that $\Omega^2 = O(1)$, where we defined $\Omega^2 \equiv (\omega R_0 / v_A)^2 / \delta$ and $\delta \equiv \gamma \beta / 2 = O(\varepsilon^2)$. Thus, keeping only leading order terms one can reduce the system of equations Eq.(9) to

$$\Omega^2 y + \delta^{-1} \partial_\parallel^2 y + 2 \sin \theta \, z = 0, \tag{10}$$

$$\Omega^2 z + \partial_\parallel^2 z + 2\Omega^2 \sin \theta \, y = 0, \tag{11}$$

where $y \equiv \xi_s \varepsilon / q$, $z \equiv \nabla \cdot \vec{\xi}$, $\partial_\parallel \equiv R_0 d/dl$ and l is the distance along the field line. For sufficiently small values of ε and β, numerical solutions of Eqs.(9,11) are found to be almost identical to accurate numerical solutions of NOVA code [14], which also solves Eqs.(9).

One can see that two equations, Eqs.(9,11), are coupled due to the finite compressibility of the toroidal plasma. The coupling of acoustic or Alfvénic branches with the dominant poloidal mode number m is via the $m \pm 1$ sideband harmonics of the other branch. The result of such coupling is shown as Alfvén-acoustic continuum in Fig. 2b. It is seen from this figure that the continuum curves break and the continuum gaps emerge. The presence of such gaps is remarkable. In fact, they open up a possibility for global weakly damped contained eigenmodes to exist without the interaction with the continuum.

It was also found that the Alfvén-acoustic solutions are difficult to treat analytically because the small parameters are not readily found [17]. In those cases one has to rely on

5

numerical solutions, such as to consider the coupling of higher order poloidal harmonics, $m \pm 2$ and so on. In realistic plasmas the shift to the mode frequency can be on the order of local plasma β, which can be a fraction of unity.

In this paper we present the key points with the Alfvénic waves without detailing the physics of its coupling to the acoustic branch[18].

B. Alfvénic gap modes and numerical solutions

The Alfvénic continuum, if existing in the region of low shear (constant q profile) and flat density profile, is consistent with the regions of the global solutions. Because the rigorous formulation is beyond the scope of this paper we show some of the results and derivations only schematically. With this goal in mind we write the Alfvén equation for a single poloidal harmonic in a cylinder

$$\frac{1}{r^2}\frac{\partial}{\partial r}r^3 R_0^2\left[k_{\parallel m}^2 - \frac{\omega^2}{v_A^2}\right]\frac{\partial}{\partial r}\frac{\phi(r,t)}{r} - \frac{m^2}{r^2}R_0^2\left[k_{\parallel m}^2 - \frac{\omega^2}{v_A^2}\right]\phi(r,t) = 0. \tag{12}$$

The analysis of this equation shows that near the continuum its solution has a logariphmic singularity in radius at a point which is give by the Alfvén frequency, Eq.(7). The radial dependence of $\omega_A(r)$ for example leads to the existence condition of the GAEs (global Alfvén eigenmodes) when $\omega_A(r)$ has a local extremum point. It was shown that its local minimum corresponds to the so-called Global Alfvén Eigenmodes (or GAE) [19, 20].

In the case where the local continuum produces gaps a new type of global solution emerges known as toroidicity-induced Alfvén eigenmodes (TAEs) [14, 16]. These modes are weakly damped and are considered one of the most probable candidate driven by the fusion alphas in a DT reactor such as ITER [21, 22].

Important properties of TAEs can be used to determine their frequency. These modes are located at the intersection of m and $m+1$ poloidal harmonics, so that $\left|k_{\parallel m}\right| = \left|k_{\parallel m+1}\right|$ and thus

$$q_{TAE} = \frac{m - 1/2}{n}. \tag{13}$$

For the TAE frequency we have then

$$\omega_{TAE} = \frac{v_A f}{2 q_{TAE} R}, \tag{14}$$

where function $f = 1 + O(\varepsilon, s)$ is the refinement correction due to finite toroidicity and magnetic shear [23]. One can see from the last equation that if we know the mode frequency we can deduce the information about the safety factor at the TAE location, which is one element of the so-called MHD spectroscopy [24]. Also an excitation of GAEs can have similar information about the local q value and can be exploited.

The following figure shows an example of the AC plotted for the ITER normal shear discharge simulated by the transport analyzing code TRANSP [25]. We indicate the location of three big gaps: BAE (beta-induced Eigenmode), TAE and EAE (ellipticity-induced Eigenmode) gaps. In ITER the continuum gap envelope radial dependence follows approximately the Alfvén frequency as the TAE gap shown in the figure. In the particular example shown the Alfvén frequency dependence is approximately $q^{-1}(r)$ because the density profile (and thus the Alfvén velocity) is almost constant.
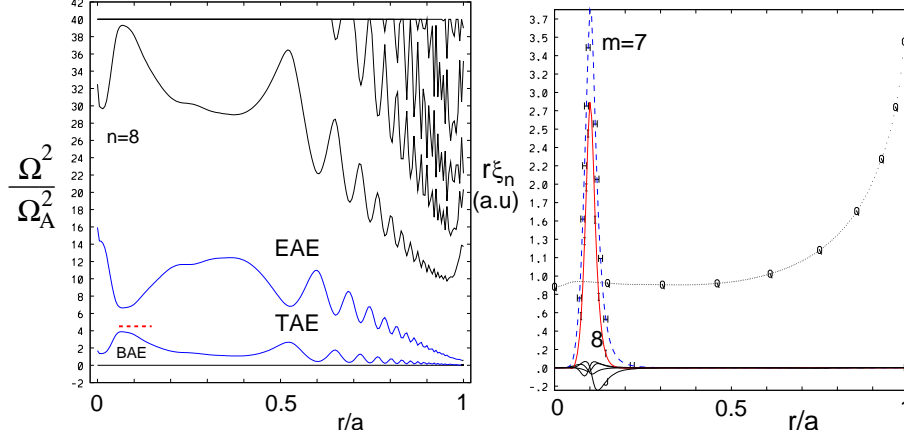
6

Figure 3: *Ideal MHD continuum for ITER normal shear H-mode plasma run #20000T02 TRANSP run and the most unstable core localized TAE poloidal harmonic radial structure for this case with NBI aiming 10cm below the magnetic axis. The radial extent of this mode is shown in the left figure as a dashed line corresponding to the normalized TAE eigenfrequency. (The figure is reproduced from Ref.[26]).*

Eigenmode structures of the aforementioned modes, TAEs, were found numerically for the ITER normal shear plasma. The eigenmodes were computed with the help of the ideal MHD NOVA code [14]. The code solves general geometry ideal MHD equations, similar to Eq.(12), but written for the set of poloidal harmonics and thus coupled together in a system. The solution found for the considered case, Fig.(3,b) is clearly showing the "classic" TAE couplet, which is characterized by two dominant poloidal harmonics. The radial width of such core-localized TAEs is narrow and determined by radial dependence of the q-profile [27], which is relatively flat near the axis.

C. Experimental validation of linear TAE theory

We realized that the energetic particle driven modes in the linear regimes are due to a higher order MHD effects, which need to be kept, in theory, in order to develop a framework to find these eigenmodes. This is arguably the most powerful tool to verify the whole MHD model. As we discussed above, such a higher order correction to the "homogeneous" approximations as geometry (toroidicity, cross-section non-circularity, etc.), plasma pressure (via coupling to the acoustic branches), FLR kinetic effects and others are therefore small, but can be rigorously tested. Perhaps the most compelling case for such tests corresponds to the excitation of *AEs (we use a generalized abbreviation for a variety of Alfvénic eigenmodes). One example of such a case corresponds to plasma with NBI driven modes in DIIID.

In DIIID a recent experimental campaign was directed at fast ion studies [28]. One key element of the studies was the use of a special diagnostic, FIDA, (fast ion D_α) spectroscopy for fast ion relaxation measurements and the electron-cyclotron-emission (ECE) diagnostic for *AE measurements. Among many reported results the authors focused on linear physics [29], which resulted in strong validation not only of the ideal MHD code NOVA but of the whole MHD theory. Together with Mirnov magnetic probes, ECE was used to identify and document several *AE modes. In addition, for each mode with the measured toroidal
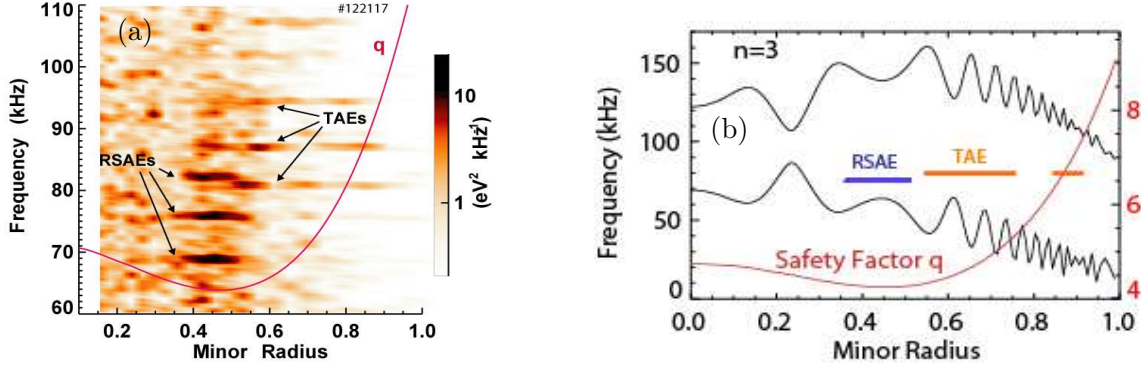
Figure 4: *DIIID results on *AE excitation by beam ions in a reversed shear plasma. Figure (a) represents the ECE signal radiometer spectrum. Figure (b) shows AC profiles with the solid lines corresponding to RSAE and TAE frequencies and their radial extend.*

mode number a numerical analysis provided the radial structure of the perturbed plasma displacement, which was in turn compared with the ECE signal.

The following figures show the results of such a comparison, which we show following publication [29]. First we show the internal signal coming from the ECE radiometer power spectra on Fig. 4a. It represents the TAE and RSAE modes, which were identified with the help of the NOVA code and additional diagnostics data. Fig. 4b shows the AC for this case with two mode frequencies indicated as horizontal lines, which are radially extended according to the mode structure.

Perhaps the most impressive data comes from the ECE radial structure of these modes and how it compares with the computed ones. Figure 5 shows the comparison for two modes, $n = 2$ RSAE and $n = 3$ TAE. The radial plasma displacement dependence with all the phase inversions can easily be seen to agree with the MHD theory. Given finite accuracy of the ECE data and other used modeling tools the agreement seems to be very impressive and important for the MHD theory in general.

One of the key and surprising conclusions of the DIIID campaign was that they did show that RSAE modes are the ones that contribute most to the EP transport. The surprise comes from a fact that the RSAEs are relatively localized modes and typically characterized by only one dominant poloidal harmonic [30]. Possibly this is due to the presence of low magnetic shear, whereas the TAEs are global and exist in a region of relatively strong shear. In the next section we address the transport issues on EPs due to the presence of *AEs.

D.   EP linear drive of *AEs

Alfvénic modes can be excited and studied in several ways. One is "natural" excitation due to the presence of superalfvénic EPs, which can be in resonance with a certain mode, such as TAE, EAE or other. Another is the external excitation of a mode via the external antennae. Typically the antennae excitation of *AEs is used to study their damping[31]. To utilize the antennae excitation further it was suggested that we control EP behavior in the phase space [32] for subsequent ash removal of the fusion products (cooled alpha particles) from a fusion plasma. One of the dependencies that mechanism relies on is the relation between the energy and the canonical momentum change during the low frequency activity,
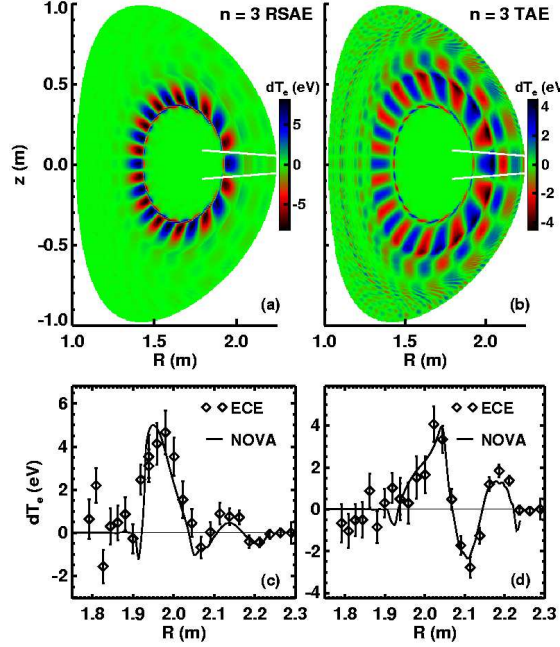
Figure 5: *Comparison of DIIID TAE and RSAE radial structures results as measured by ECE diagnostics with predictions by the NOVA code.*

which includes TAEs. It is known from a wave particle theory that it can be expressed as

$$\frac{\Delta P_\varphi}{n} = \frac{\Delta \mathcal{E}_h}{\omega}. \tag{15}$$

It follows from this expression that the low-frequency oscillations have rather low energy change whereas the high-frequency ones lead primarily to the particle energy variation. The same relation is important in the formulation of the growth rate expression.

We will write the growth rate expression of TAEs due to resonances with EPs driven by their gradient. For that we will be following the heuristic rules. First the growth rate should be proportional to the EP beta, β_h. Moreover, the drive is coming mostly from the beta gradient, and should be proportional to $n\partial \ln \beta_{EP}/\partial \ln r$, where we included Eq.(15). Because only resonant particles can effectively interact with a certain mode, the following resonant factor accounts for this $\int \frac{dv^3}{v_h^3}\delta(\omega - \omega_h)$. This is done by choosing only certain group of particles from the whole velocity space. Here, for the sake of simplicity, we present the particle characteristic wave-phase frequency as ω_h, which can be approximated as $k_\parallel v_\parallel$ in the simple case of the narrow eigenmode.

Combining together all these factors we can find that the drive should be proportional to

$$\frac{\gamma_h}{\omega} \simeq \beta_h \frac{n\partial \ln \beta_h}{\partial \ln r} \int \frac{dv^3}{C v_h^3}\delta\left(\omega - k_\parallel v_\parallel\right), \tag{16}$$

where in addition we introduced a normalization/correction constant C.

In the last expression we presented the so-called universal, gradient drive. We left velocity and anisotropy contributions out of the consideration [3], which are important especially in the interpretation of the experimental data [5]. A more complete expression for the growth
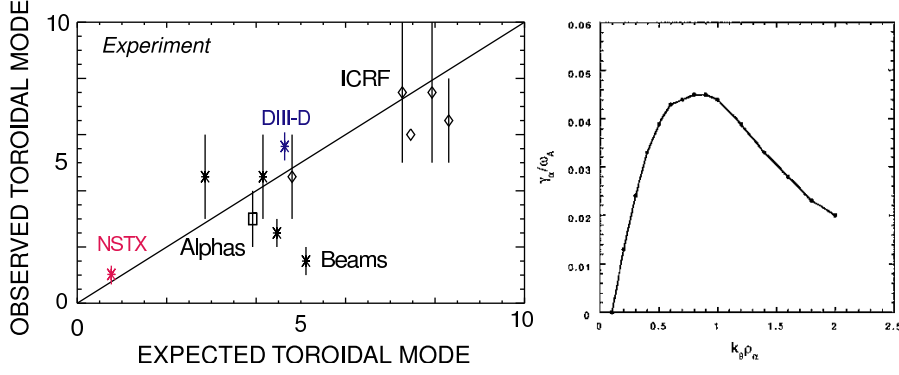
9

Figure 6: *Experimental evidence for the predictions of the most unstable mode number scaling TAEs from DIIID/NSTX similarity experiments [34].*

rate does include those effects, which we present in the following form without the derivation (see for example [33])

$$\frac{\gamma_h}{\omega} = \beta_h \int \frac{dv^3}{Cv_h^3} \delta\left(\omega - k_\parallel v_\parallel\right) \left[-\omega + \frac{m}{\omega_{ch}} \frac{\partial \ln \beta_h}{\partial \ln r}\right] f\left(v_{res}\right) \frac{1}{\Delta_h/\Delta_m + 1}. \tag{17}$$

One important addition to the growth rate expression here accounts for the finite width of the EP drift orbits. It does not change the growth rate expression if the mode number is small, i.e. $\Delta_m = r^2/msR \gg \Delta_h = q\rho_h$, where ρ_h is the Larmor radius of EP, and eliminates the growth rate mode number $n-$dependence at $\Delta_m \sim \Delta_h$, i.e., when this expression reaches maximum value. We would like to note that Δ_h/Δ_m dependence of the growth rate is practically important for a fusion reactor design as it plays a stabilizing role reducing and limiting γ_h/ω dangerous growth. Such a limitation is being speculated to benefit burning plasmas [21].

It seems fairly important to show the observed proofs of the last point following from the similarity experiments on DIIID and NSTX. In those experiments the plasmas were set up in a similar way but with different major radii. Fig. 6(a) represents these results, which include a variety of experiments with NBI, ICRH, fusion alphas on DIIID, as well as with beam ions on NSTX. Because the toroidal number of the most unstable mode satisfies the condition $\Delta_h/\Delta_m = 1$ one can find that it requires $n \simeq r/\rho_h q^2$ [33]. Expected versus observed mode numbers are shown as points on that figure. The main effect in those experiments was due to the difference in DIIID and NSTX q factor.

Theory predicts this dependence by analyzing the orbit width effect on the TAE drive using several methods. In one work the authors made use of the high-n ballooning formalism, which resulted in the growth rate plato at $k_\theta \rho_h \simeq 1$. This resulting dependence is reproduced in Fig. 6(b).

The same theory serves as a baseline for predictive simulations of TAE stability performed for ITER plasma. As expected, these results shift the range of unstable mode numbers to relatively high values of $n = 5 - 15$. We would like to show the example of the TAE range frequency modes growth rates as a function of n (see figure 3). In the shown results we have chosen a case with the most unstable modes characterized by highest growth rates.

Later an international group of EP physics experts attempted to compare the computer codes computations and found an excellent agreement in the mode structure of TAEs and in the computed radiative and continuum damping rates among them [35].

IV. NONLINEAR RELAXATION OF FAST ION PROFILES

We considered a relatively simple way of treating the confined EPs in a plasma close to burning conditions, which is aimed at treating the fast ion profiles beyond the linear physics. For that we rely on the arguably the one of the most successful and verified part of the EP physics, which is the linear physics of *AE instabilities.

First, here is an outline the quasilinear theoretical model [36]. Several elements of linear theory are of use. One is that the mode damping due to the background components is relatively constant. It is assumed to be fixed in the model described hereafter. The second assumption is that the instability is characterized by many modes, sometimes called a "sea" of modes. This is required by the quasilinear theory for the diffusion process to be applicable on a global scale of the plasma cross-section. We also assume that EPs are moving quickly within the unstable domain, which is the flattening region of EP density near the resonance. This way we can ignore any dynamics of the EP-plasma system due to the nonlinear physics.

Qualitatively, the formulation of the redistribution of EPs can be described in the following way. We balance the linear drive with the background damping locally at each radial point. The first one, drive, is assumed to be proportional to the gradient of fast ion pressure, $\gamma_L \propto \partial \beta_h / \partial r$. Subsequently, the mode should grow at a rate $\gamma = \gamma_L + \gamma_{damp}$ where γ_{damp} is the background plasma damping. The fast ions are redistributed and their growth rate contribution diminishes until it becomes comparable to the damping rate at which stage the marginal stability is achieved. As a result of such a balance the critical EP pressure gradient emerges and the value of the damping gives the expression for the "critical" pressure gradient. It can be mixed over the velocity space between the resonant and non-resonant particles and integrated in radius to find the relaxed EP pressure profile.

The phase space diffusion near each resonance can be due to either particle-wave phase mixing or to multiple mode resonance overlapping. It is reasonable to expect one of those mechanisms present in the system given the assumption of high numbers of unstable modes.

We also should note that applying the growth rate expression we find the critical pressure gradient including the resonant particles in an analytic form. Thus, having in mind that the radial pressure dependence is being modified and the fact that the velocity distribution is being only partially accounted for, this model is called the $1.5D$ quasilinear relaxation model.

We should say that the nonlinear saturation dynamics may be important, especially for the details of the EP profile relaxation, such as its temporal evolution. However, for a reactor it seems sufficient to propose a model which captures basic linear physics to establish the EP profile evolution [37]. With that purpose in mind the experimental validation of the proposed model was performed and is being prepared for publication [*ibid*].

A. 1.5D quasilinear model formulation

The $1.5D$ quasilinear fast ion profile relaxation model develops a certain methodology to assess the instability case to determine whether or not there is likely to be a substantial loss of energetic particles due to diffusion from the fields generated by the TAE modes. In the rest of this section we follow this methodology and the model description as given in Ref.[36].

The local critical alpha particle pressure gradient within this theory can be estimated from the balance between the drive and the dissipative mechanisms, which were ion Landau

damping, γ_{iL}, and trapped electron collisions, γ_{ecoll} [38]. Indeed, it was shown that these two damping mechanisms are dominant for the expected radial location of the medium mode number, unstable TAEs at $r/a \geq 0.5$. Equating driving and damping terms reads,

$$\frac{\partial \beta_{hcr}}{\partial r} = -\frac{\gamma_{damp}}{\gamma\prime_h}, \tag{18}$$

where $\gamma_h\prime = \gamma_h / (\partial \beta_h / \partial r)$. The right side of this equation is independent on β_h and depends on the background plasma parameters. In our $1.5D$ model we consider a one dimensional quasi-linear equation where the spatially local diffusion coefficient, $D(r)$, grows at a rate proportional to $\gamma_h + \gamma_{iL} + \gamma_{ecoll}$.

The diffusion coefficient growth when the instabilities set up relaxes the critical EP pressure gradient and may increase the size of the surrounding stable region. The net result is the relaxation of the distribution function to a marginally stable one over a region that is larger than the original instability region. Consequently, this model makes a prediction for the amount of redistribution and transport of the alpha particles, without performing the complicated calculations of obtaining the perturbed fields that produce the diffusion coefficient.

The model assumes that initially an unstable region lies in a single radial band. It is expected that the alphas beta profile flattens beyond the unstable region of linear theory and a relaxed (denoted as rlx) alpha particle beta profile $\beta_{hrlx}(r)$ forms. The quasi-linear theoretical model predicts that the original unstable region spreads in space to satisfy the condition, $\partial \beta_{hrlx}/\partial r = \partial \beta_{hcr}/\partial r$ in a region $r_1 < r < r_3$ and at these interfaces, $\beta_{hrlx}(r_{1,3}) = \beta_h(r_{1,3})$. We need to find both r_1 and r_3, which lie within the boundaries of the plasma.

In the relaxed state the beta profile remains unmodified outside the relaxed region, while the beta profile is at marginal stability within the relaxed region. Hence within the relaxed region we find $\beta_{hrlx}(r) = \beta_h(r_1) + \int_{r_1}^{r} (\partial \beta_{hcr}/\partial r') dr'$. As $\beta_{hrlx}(r_3) = \beta_h(r_3)$, one of the conditions to determine the endpoints is, $\beta_h(r_3) - \beta_h(r_1) = \int_{r_1}^{r_3} (\partial \beta_{hcr}/\partial r') dr'$.

We note that the actual energy density that is redistributed is smaller than the above estimate [2]. Only a part of alpha particle fraction, η, undergoes redistribution due to the resonant interaction. This fraction was estimated $\eta = (v_{h0} - v_\parallel) v_\parallel / v_{h0}^2 \leq 0.25$ for the straight cylinder geometry [2, 39], where $v_\parallel$ is particle parallel velocity resonant with TAE. In the relaxation region the beta profile of alphas is then $\hat{\beta}_h(r) = \eta \beta_{hrlx}(r) + (1 - \eta) \beta_h(r)$. The resulting alpha profile is then given by
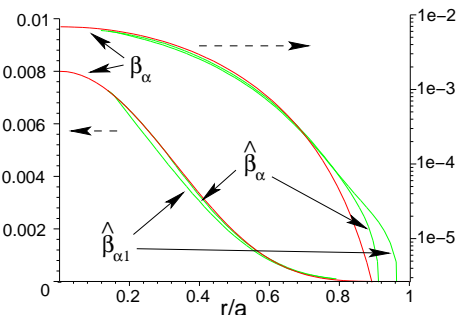

Figure 7: *Alpha beta profiles initial and reconstructed using Eq.(18). Profile $\hat{\beta}_{h1}$ is obtained for critical beta from Eq. (18) multiplied by 0.7. Profiles are shown in linear and logarithmic scales.*

$$\hat{\beta}_h(r) = \begin{cases} \beta_h(r), \ r < r_1 \\ \eta \beta_{hrlx}(r) + (1 - \eta) \beta_h(r), \ r_1 < r < r_3 \\ \beta_h(r), \ r > r_3 \end{cases} \tag{19}$$

In this section we also demonstrate the application of $1.5D$ quasilinear model to a burning ITER-like plasma with the parameters based on the TRANSP calculations. Steady-state beta profile of alphas can be fitted closely to $\beta_h = 0.008 \left[1 - (r/a)^2\right]^5$. Another important profile is the plasma

ion temperature profile taken as $T_i(keV) = 20\left[1 - (r/a)^2\right]$, while the background beta is $\beta_{pc} = 0.06\left[1 - (r/a)^2\right]$. We apply the relaxation of the beta profile with $\eta = 0.25$ and show it in Fig. 7.

For this case shown on Fig.7, TAEs are locally unstable within $0.39 < r/a < 0.72$. After the quasi-linear transport model is applied, alphas are redistributed within a wider domain, $r_1/a = 0.30 < r/a < r_3/a = 0.89$, (see curve marked with $\hat{\beta}_h$) in Fig. 7. After EP redistribution, the growth rate in our model equals the damping rate and by making use of the result of Ref.[38] is $\gamma_h = -\gamma_{iL} - \gamma_{ecoll} = 4\%$ at the most unstable point, $r/a \simeq 0.6$. At this point we have $s = 0.3$, $q = 1.5$, $T_i = 12keV$ ($T_{i0} = 20keV$). This compares with the growth rate before the redistribution $\gamma_h \simeq 4.7\%$ for the same background plasma.

Stronger radial transport is expected if the thermal ion temperature is raised because fusion alpha-particle beta depends on T_i: $\beta_h/\beta_{pc} = \sigma^2 0.117 T_i^{5/2}/(1 + \sigma)$, where $\sigma \equiv (n_D + n_T)/n_e = 0.8$. Figure 8 shows the expected loss dependence with increased alpha particle beta as the temperature was increased from a baseline case of $T_{i0} = 20keV$, $\beta_{pc0} = 6\%$, and $\beta_{h0} = 0.8\%$. Here, in one case, the plasma density is fixed (solid curve) and in another case, the plasma beta (dashed curve) is, while keeping fixed $r_3 = a$. In the case of fixed plasma density the predicted TAE induced transport is weaker because the ion Landau damping is increasing with ion temperature. With the constant beta, the ion temperature was varied from $20\,keV$ at $\beta_{h0} = 0.8\%$ to $\sim 24\,keV$ at
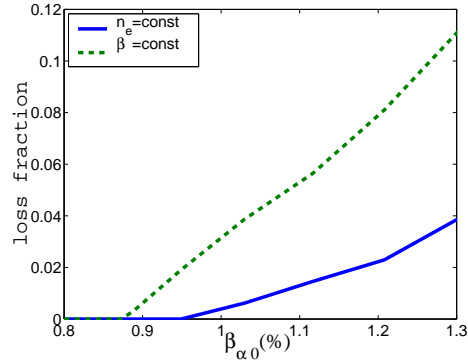

Figure 8: *Expected alpha particle losses are shown as fa unction of increased $\beta_{\alpha 0}$ keeping fixed total plasma beta (dashed, $\beta \equiv \beta_{pc} + \beta_{\alpha h} = $ const, $\beta_{h0} \sim T_{i0}^{5/2}$) and density (solid, $\beta_{h0} \sim T_{i0}^{7/2}$).*

$\beta_{h0} = 1.3\%$, whereas at fixed density the corresponding temperature range was from $20keV$ to $\sim 23keV$. We see that losses can become severe with increased temperature especially for the fixed beta case.

In the calculations in this section the quasilinear relaxation model neglects the TAE interaction with beams assuming that only one specie is driving the instability. It seems possible to renormalize the critical gradients proportional to the contribution of each specie to the total drive. The proposed model needs to be corrected by numerical calculations to account for extra damping mechanisms. More detailed investigations can be adjusted to numerically evaluated damping and growth rates, as obtained in NOVA-K simulations. The outlined model shows that in the case of local instability theory the TAE instability effects allow window of operation in ITER, but will establish the high-temperature limits.

V.   SUMMARY

We demonstrated several key successes of EP physics in fusion research. Most of them are directly applicable to ITER and in general to burning plasmas. They span from single particle confinement, excitation of the low frequency Alfvénic modes, to the nonlinear saturation of these modes and so on.

A specific example of EP physics progress seems to be fairly important to note separately, which is the confirmation of MHD theory in general. These models are built on higher order corrections to ideal homogeneous plasma MHD and their effects due to the plasma toroidicity, non-circularity of the cross section, finite plasma pressure and so on. This confirmation is coming primarily from the comparison of the mode structure and their stability.

There are several remarks we would like to make here to help summarize the presented material. One is that it is of great importance to have accurate estimates of the damping and growth rates to understand the stability properties of EP driven modes and their effect on plasma performance. However, if one makes plans to build a fusion reactor, it is not necessary to do the estimates too accurately for all the modes. One has to develop a model which would capture the parameter dependencies accurately and be qualitatively correct. In the example of the quasilinear model we saw that it can predict the profiles of EPs, but lacks certain observable features. Nevertheless, it can be applied for future devices. In fact, such application to experiments on DIIID are being done in order to validate its predictive capabilities [37].

The qualitative estimate for the damping/driving rates is often enough to validate the use of a certain EP theory. In cases when prediction has to be quantitatively efficient, the stability model has to be corrected by more advanced accurate tools.

[1] L. V. Korablev and L. I. Rudakov, Zh.Eksp.Teor.Fiz. (Sov. Journal Exp. Theor. Phys.) **54**, 818 (1968).

[2] Y. I. Kolesnichenko, Nucl. Fusion **20**, 727 (1980).

[3] A. B. Mikhailovskii, **9**, 103 (1986).

[4] S. V. Putvinskij, **18**, 239 (1993).

[5] W. W. Heidbrink and G. J. Sadler, Nucl. Fusion **34**, 535 (1994).

[6] K. L. Wong, Plasma Phys. Control. Fusion **41**, R1 (1999).

[7] B. N. Breizman and S. E. Sharapov, Plasma Phys. Control. Fusion **53**, 054001 (2011).

[8] Y. I. Kolesnichenko, A. Könies, V. V. Lutsenko, and Y. V. Yakovenko, Plasma Phys. Control. Fusion **53**, 024007 (2011).

[9] G. Vlad, F. Zonca, and S. Briguglio, Riv. Nuovo Cimento **22**, 1 (1999).

[10] N. N. Gorelenkov, R. Budny, H. Duong, R. Fisher, S. Medley, M. Petrov, and M. Redi, Nucl. Fusion **37**, 1053 (1997).

[11] S. S. Medley, D. K. Mansfield, A. I. Roquemore, R. K. Fisher, H. H. Duong, J. M. McChesney, P. B. Parks, M. P. Petrov, A. V. Khudoleev, and N. N. Gorelenkov, Rev. Sci. Instrum. **67**, 3122 (1996).

[12] Y. I. Kolesnichenko and V. N. Oraevski, Atomnaya energy (Sov. Atomic Energy v.23 (1967) 1028) **23**, 289 (1967).

[13] J. P. Goedbloed, Phys. Fluids **18**, 1258 (1975).

[14] C. Z. Cheng and M. S. Chance, Phys. Fluids **29**, 3695 (1986).

[15] N. N. Gorelenkov, H. L. Berk, E. Fredrickson, and S. E. Sharapov, Phys. Lett. A **370/1**, 70 (2007).

[16] C. Z. Cheng, Phys. Reports **211**, 1 (1992).

[17] A. I. Smolyakov, C. Nguyen, and X. Garbet, Plasma Phys. Control. Fusion **50**, 115008 (2008).

[18] N. N. Gorelenkov, M. A. Van Zeeland, H. L. Berk, N. A. Crocker, D. Darrow, E. Fredrickson, G.-Y. Fu, W. W. Heidbrink, J. Menard, and R. Nazikian, Phys. Plasmas **16**, 056107 (2009).

[19] S. M. Mahajan and D. W. Ross, Phys. Fluids **26**, 2195 (1983).

[20] Y. M. Li, S. M. Mahajan, and D. W. Ross, Phys. Fluids **30**, 1466 (1987).

[21] N. N. Gorelenkov, H. L. Berk, R. V. Budny, C. Z. Cheng, G. Y. Fu, W. W. Heidbrink, G. J. Kramer, D. Meade, and R. Nazikian, Nucl. Fusion **43**, 594 (2003).

[22] A. Fasoli, C. Gormezano, H. L. Berk, B. Breizman, S. Briguglio, D. S. Darrow, N. Gorelenkov, W. W. Heidbrink, A. Jaun, S. V. Konovalov, et al., Nucl. Fusion **47**, S264 (2007).

[23] G. Y. Fu, Phys. Plasmas **2**, 1029 (1995).

[24] E. Joffrin, A. C. C. Sips, J. F. Artaud, A. Becoulet, L. Bertalot, R. Budny, P. Buratti, P. Belo, C. Challis, F. Crisanti, et al., Nucl. Fusion **45**, 626 (2005).

[25] R. V. Budny, Nucl. Fusion **42**, 1383 (2002).

[26] N. N. Gorelenkov, H. L. Berk, R. V. Budny, C. Kessel, G. Kramer, D. McCune, J. Manickam, R. Nazikian, and A. Polevoi, Preprint: PPPL- **4287** (2008).

[27] H. L. Berk, J. W. Van Dam, D. Borba, J. Candy, G. T. A. Huysmans, and S. Sharapov, Phys. Plasmas **2**, 3401 (1995).

[28] W. W. Heidbrink, N. N. Gorelenkov, Y. Luo, M. A. Van Zeeland, R. B. White, M. E. Austin, K. H. Burrell, G. J. Kramer, M. A. Makowski, G. R. McKee, et al., Phys. Rev. Lett. **99**, 245002 (2007).

[29] M. A. Van Zeeland, G. J. Kramer, M. E. Austin, R. L. Boivin, W. W. Heidbrin, M. A. Makowski, G. R. McKee, R. Nazikian, W. M. Solomon, and G. Wang, Phys. Rev. Letters **97**, 135001 (2006).

[30] S. E. Sharapov, B. Alper, H. L. Berk, D. N. Borba, B. N. Breizman, C. D. Challis, A. Fasoli, N. C. Hawkes, T. C. Hender, J. Mailloux, et al., Phys. Plasmas **9**, 2027 (2002).

[31] A. Fasoli, D. Borba, G. Bosia, D. J. Campbell, J. A. Dobbing, C. Gormezano, J. Jacquinot, P. Lavanchy, J. B. Lister, P. Marmillod, et al., Phys. Rev. Lett. **75**, 645 (1995).

[32] N. J. Fisch and J.-M. Rax, Phys. Rev. Lett. **69**, 612 (1992).

[33] H. L. Berk, B. N. Breizman, and H. Ye, Phys. Lett. A **162**, 475 (1992).

[34] W. W. Heidbrink, E. D. Fredrickson, N. N. Gorelenkov, A. W. Hyatt, G. J. Kramer, and Y. Luo, Plasma Phys. Control. Fusion **45**, 983 (2003).

[35] D. Borba, A. Fasoli, N. N. Gorelenkov, S. Gunter, P. Lauber, N. Mellet, R. Nazikian, T. Panis, S. D. Pinches, D. Spong, et al., in *Proceedings of 23rd IAEA Fusion Energy Conference, Daejeon, Republic of Korea* (2010), THW/P7-08, pp. 1–8.

[36] N. N. Gorelenkov, H. L. Berk, and R. V. Budny, Nucl. Fusion **45**, 226 (2005).

[37] K. Ghantous, N. N. Gorelenkov, and M. V. Zeeland, In preparations (2012).

[38] N. N. Gorelenkov, E. D. Fredrickson, E. Belova, C. Z. Cheng, D. Gates, S. Kaye, and R. B. White, Nucl. Fusion **43**, 228 (2003).

[39] V. S. Belikov and Y. I. Kolesnichenko, Fusion Technol. **25**, 258 (1994).

The Princeton Plasma Physics Laboratory is operated
by Princeton University under contract
with the U.S. Department of Energy.

Information Services
Princeton Plasma Physics Laboratory
P.O. Box 451
Princeton, NJ 08543

Phone: 609-243-2245
Fax: 609-243-2751
e-mail: pppl_info@pppl.gov
Internet Address: http://www.pppl.gov